ANTIOXIDANTS & REDOX SIGNALING
Volume 9, Number 12, 2007

DOI: 10.1089/ars.2007.1797

Forum Original Research Communication

A$\beta_{1\text{-}42}$ Induces Mild Endoplasmic Reticulum Stress in an Aggregation State–Dependent Manner

SIDHARTHA M. CHAFEKAR,[1] JEROEN J. M. HOOZEMANS,[1,3] ROB ZWART,[1] FRANK BAAS,[1,2] and WIEP SCHEPER[1,2]

ABSTRACT

Alzheimer's disease (AD) is characterized by the aggregation of misfolded proteins. Previously we reported activation of the unfolded protein response (UPR) in AD neurons. A potential source for UPR activation in AD neurons may be the increased levels of β-amyloid (Aβ). In this study, we used preparations enriched in oligomeric or fibrillar A$\beta_{1\text{-}42}$ to investigate the role of the conformational state of Aβ in UPR activation in differentiated neuroblastoma cells. Both oligomeric and fibrillar A$\beta_{1\text{-}42}$ do not induce BiP expression to the extent that it can be detected in a pool of cells. However, using a fluorescent UPR reporter cell line that allows analysis of individual cells, we demonstrated mild activation of the UPR by oligomeric but not fibrillar A$\beta_{1\text{-}42}$. We showed that oligomeric A$\beta_{1\text{-}42}$ is significantly more toxic to cells primed for UPR than is fibrillar A$\beta_{1\text{-}42}$, indicating that activation of the UPR contributes to oligomer-specific A$\beta_{1\text{-}42}$ toxicity. Because UPR activation is observed in AD brain at a stage that precedes the massive fibrillar Aβ deposition and tangle formation, this may indicate a role for nonfibrillar Aβ in the induction of the UPR in AD neurons. *Antioxid. Redox Signal*. 9, 2245–2254.

INTRODUCTION

Alzheimer's disease (AD) is neuropathologically characterized by the accumulation of aggregated proteins: intracellular aggregates of hyperphosphorylated tau in the neurofibrillary tangles and extracellular aggregates of β-amyloid (Aβ) in the senile plaques (15). Therefore, AD is a prime example of a protein-folding disease.

Accumulation of aggregation-prone proteins in the endoplasmic reticulum (ER) triggers a cellular stress response called the unfolded protein response (UPR) (5, 17). Under normal cellular homeostasis, the ER chaperone BiP (or GRP78) is bound to three sensor proteins at the ER membrane; pancreatic ER kinase (PERK), transcription factor ATF-6, and endoribonuclease Ire-1. Increased levels of unfolded proteins titrates BiP from the sensor proteins, which are consequently activated. UPR activation results in (a) transcriptional induction of ER chaperones, including BiP, to increase the protein-folding capacity of the ER and prevent protein aggregation; and (b) translational attenuation to reduce protein overload in the ER.

Recently, we and others showed the activation of the UPR in neurons in AD brain (9, 19). In the temporal cortex and hippocampus of AD patients, protein levels of BiP are increased compared with those in nondemented control cases. In addition, phosphorylated PERK is found in neurons of AD patients, but not in nondemented control cases. BiP/GRP78 expression levels were shown to increase progressively with increasing Braak scores for amyloid deposits. A potential source for the activation of the UPR in AD could thus be an increase in Aβ levels. *In vitro* studies indicate that Aβ toxicity involves the ER stress response. Knockdown of BiP increases cell death induced by A$\beta_{25\text{-}35}$ in rat hippocampal neurons (18, 22), indicating that the ER chaperone BiP protects against Aβ toxicity. Aβ appears to activate ER-stress–specific caspases: Aβ-induced cytotoxicity

[1]Neurogenetics Laboratory and [2]Department of Neurology, Academic Medical Center, University of Amsterdam, and [3]Department of Pathology, VU University Medical Center, Amsterdam, The Netherlands.

is reduced in caspase-12–deficient cortical mouse neurons (16). The human homologue of caspase-12, caspase-4, is also activated by Aβ (6). Together, these data point toward a role for ER stress in the cellular response to Aβ, although actual activation of the UPR by Aβ has not been demonstrated. In this study, we investigated the role of the conformational state of Aβ in ER stress induction. The data presented here show that A$\beta_{1\text{-}42}$ does not induce upregulation of BiP, irrespective of the aggregation state. However, using a fluorescent ER stress indicator that allows analysis of individual cells, we demonstrated mild activation of the UPR by oligomeric but not fibrillar A$\beta_{1\text{-}42}$. Moreover, we demonstrated that activation of the UPR contributes to oligomer-specific A$\beta_{1\text{-}42}$ toxicity *via* an apoptotic mechanism, indicating that UPR activation might be one of the molecular mechanisms responsible for oligomer-specific Aβ toxicity.

MATERIALS AND METHODS

Cell culture, constructs, and transfections

Cell-culture reagents were purchased from Gibco BRL (Gaithersburg, MD). SK-N-SH human neuroblastoma cells were maintained in DMEM supplemented with 10% fetal calf serum (FCS), 100 U/ml penicillin, 100 μg/ml streptomycin, and 300 μg/ml glutamine.

SK-N-SH human neuroblastoma cells were differentiated for 5 days using cell-culture medium supplemented with 10 μM retinoic acid (Sigma, St. Louis, MO), before treatment with A$\beta_{1\text{-}42}$ treatment for 48 h in cell-culture medium without phenol red. HEK293 cells stably expressing the ERAI fluorescent reporter plasmid pCAX-F-XBP1deltaDBD-venus [a kind gift from Dr. M. Miura, Tokyo, Japan (11)] were obtained by cotransfection with pcDNA3 using lipofectamine 2000 (Invitrogen, Carlsbad, CA), according to manufacturer's protocols. Separate colonies were selected using 500 μg/ml G418 (Invitrogen), and expression of the ERAI reporter was established by the appearance of fluorescent cells on treatment with 0.2–1 μg/ml tunicamycin (Sigma) for 24 h. The stable ERAI cells were maintained in the same medium as SK-N-SH cells supplemented with 50 μg/ml G418.

Peptide solubilization and aggregation

To obtain A$\beta_{1\text{-}42}$ preparations enriched in oligomers and fibrils, we essentially used the method described by Dahlgren *et al*. (1). A$\beta_{1\text{-}42}$ or A$\beta_{42\text{-}1}$ peptide (Anaspec, San Jose, CA) was initially dissolved in 1,1,1,3,3,3-hexafluoroisopropanol (Sigma) (1mg/ml), to monomerize preexisting aggregates. Subsequently, the peptide was resuspended in anhydrous dimethyl sulfoxide (DMSO) to a concentration of 2.5 m*M* and bath sonicated for 10 min. To enrich for oligomers, phenol red–free DMEM was added under continuous vortexing to bring the peptide to a final concentration of 100 μM and incubated at 4°C for 24 h. To enrich for fibrils, 10 m*M* HCl was added under continuous vortexing to bring the peptide to a final concentration of 100 μM and incubated for 24 h at 37°C. The fibrillar A$\beta_{1\text{-}42}$ preparation was centrifuged (220,000 *g*) in a Beckman tabletop ultracentrifuge for 30 min at room temperature, and the pellet was resuspended in 4% DMSO/10 m*M* HCL. A Bradford protein assay (Biorad, Hercules, CA) was performed on both oligomeric and fibrillar A$\beta_{1\text{-}42}$ preparations. Characterization of the A$\beta_{1\text{-}42}$ aggregates was performed by electron microscopy (EM) and thioflavin T assay. The maximal final concentration in the assays was 0.4% DMSO in the oligomeric preparations and 0.4%/1 m*M* HCl in the fibrillar preparations. These solvent concentrations were experimentally tested and do not affect any of the structural or cellular readouts.

Electron microscopy

A$\beta_{1\text{-}42}$ preparations were adsorbed onto Formvar-coated 300-mesh copper grids for 5 min, and excess fluid was filtered off. Subsequently, the samples were stained with 1% uranyl acetate for 5 min, excess fluid was filtered off, and the grids were analyzed with a Philips EM-420 transmission EM operated at 100 kV. The grids were thoroughly examined to make an overall evaluation of the structures present in the sample.

Thioflavin T fluorescence assay

A 100 μM aqueous solution of thioflavin T (ThT) was prepared and filtered through a 0.2-μm filter. For ThT measurements, A$\beta_{1\text{-}42}$ preparations (5 μM), were prepared in 10 μM ThT/90 m*M* glycine (pH 8.5) solution. Fluorescence was measured in 96-well plates using a Fluostar microplate reader (BMG Labtech GmbH, Offenburg, Germany) at an excitation wavelength of 450 nm and an emission wavelength of 485 nm.

MTT assay

The cytotoxicity of the A$\beta_{1\text{-}42}$ preparations was assessed by the 3-(4,5-dimethylthiazol-2-yl)-2,5-diphenyltetrazolium bromide (MTT) assay. Differentiated SK-N-SH cells were incubated with 10 μM oligomeric or fibrillar A$\beta_{1\text{-}42}$ preparations for 48 h. Cells were incubated with MTT (0.25 mg/ml) for 2 h at 37°C, and the formazan-salt generated by viable cells as a result of conversion of MTT was dissolved in DMSO, and the absorbance was measured at 570 nm. In some experiments, differentiated SK-N-SH cells were coincubated with 1 μM A$\beta_{1\text{-}42}$ and 0.1 μg/ml tunicamycin for 48 h.

Western blot analysis

For cell lysates, SK-N-SH cells were scraped in ice-cold lysis buffer (1% Triton X-100, 1 μg/ml leupeptin, 1 m*M* AEBSF in PBS). The total lysate (supernatant) was obtained after centrifugation at 12.000 *g* at 4°C for 5 min. Protein concentration was determined with a Bradford protein assay. Equal amounts of protein were analyzed on 8% SDS-PAGE gels and blotted onto PVDF membrane using a semi-dry electroblotting apparatus. Blots were preincubated with Blotto [5% nonfat dried milk in PBST (0.05% Tween-20 in PBS)] for 1 h and subsequently incubated with goat polyclonal anti-BiP/Grp78 antibody (Santa Cruz Biotechnology, Santa Cruz, CA) for 2 h at room temperature in Blotto. Alternatively, blots were incubated with rabbit anti-eukaryotic elongation factor 2α (eEF2α) antibody (Cell Signaling Technology, Beverly, MA)

in PBS, 5% BSA, and 0.1% Tween-20. The blots were washed 4 times in PBST and incubated for 1 h with HRP-conjugated goat anti-rabbit or rabbit anti-goat IgGs (Dako, Glostrup, Denmark). Blots were washed 4 times in PBST and once in PBS before analysis using Lumi-Light^{PLUS} Western blot substrate from Roche Diagnostics (Mannheim, Germany) and a LAS-3000 luminescent image analyzer [Fuji Photo Film (Europe) GmbH, Düsseldorf, Germany]. Western blot data were evaluated and quantified using Advanced Image Data Analyzer (AIDA, version 3.45.039; Raytest GmbH, Straubenhardt, Germany).

Immunofluorescence microscopy

HEK293 ERAI cells were grown on precoated (poly-L-lysine and laminin) glass coverslips and treated with 10 μM of either oligomeric or fibrillar A$\beta_{1\text{-}42}$ preparations for 48 h. Subsequently the cells were washed and then fixed with 4% paraformaldehyde in PBS for 20 min at room temperature. Coverslips were incubated with DAPI to visualize nuclei, washed and mounted in Vectashield (Vector Laboratories, Burlingame, CA), before analysis on a fluorescence microscope (Olympus AH3 Vanox) equipped with a digital CCD camera. Activation of the UPR results in a fluorescent signal. As a positive control, cells were treated for 24 h with 0.2–0.5 μg/ml tunicamycin. Slides were analyzed using identical exposure times for the different conditions. Pictures were taken at $\times$20 magnification. Image analysis was performed with ImagePro Plus software (Media Cybernetics, Inc.). Four fluorescence-intensity thresholds were set using the YFP fluorescence in a field of 0.5 μg/ml tunicamycin-treated cells. These thresholds were applied in all subsequent analyses. The lowest threshold (TH1) was set such that nontreated cells showed no positivity; the highest threshold (TH4) was determined using the strongest positive signal in the 0.5-μg/ml tunicamycin–treated cells, and two additional intermediate thresholds (TH2 and TH3) were chosen. The fluorescence area with intensity greater than or equal to threshold was determined for TH1-4 and normalized against the DAPI fluorescence to correct for cell numbers. This TH1 value represents the total normalized fluorescence area (tNFA). To evaluate the intensity distribution, the tNFA was subdivided in NFAs designated low (TH2-TH1), low-medium (TH3-TH2), medium-high (TH4-TH3), and high (TH4).

TUNEL assay

Differentiated SK-N-SH cells were grown on precoated (poly-L-lysine and laminin) glass coverslips and treated with 1–10 μM oligomeric or fibrillar A$\beta_{1\text{-}42}$ preparations for 48 h in the presence or absence of 0.1-μg/ml tunicamycin. Subsequently the cells were washed and then fixed with 4% paraformaldehyde in PBS for 20 min at room temperature. Coverslips were counterstained with anti-Calnexin Rabbit polyclonal antibody (Calbiochem, San Diego, CA), followed by goat anti-rabbit Cy3 (Jackson Immunoresearch, New Market, Suffolk, U.K.) and TUNEL staining using the In Situ Cell Death Detection Kit (Roche Diagnostics) according to the protocol of the manufacturer and mounted in Vectashield, before analysis on the fluorescence microscope.

Statistical methods

SPSS 12.0.1 for Windows was used to assess the statistical significance of differences between levels of toxicity on treatment with A$\beta_{1\text{-}42}$ peptides, combinations of A$\beta_{1\text{-}42}$ with tunicamycin, or medium alone. Analysis of variance (ANOVA), followed by Bonferroni's *post hoc* test, was used to analyze repeated-measures data. Student's *t* test was performed on the fluorescence-quantification data to assess statistical significance of the difference between levels of fluorescence after treatment with oligomeric or fibrillar Aβ preparations.

RESULTS

Characterization of enriched oligomeric and fibrillar A$\beta_{1\text{-}42}$ preparations

To investigate the possible differential effect of oligomeric A$\beta_{1\text{-}42}$ and fibrillar A$\beta_{1\text{-}42}$, we generated enriched preparations of oligomeric and fibrillar A$\beta_{1\text{-}42}$ as described in Materials and Methods. The A$\beta_{1\text{-}42}$ preparations were characterized by electron microscopy (EM) and thioflavin T (ThT) assay. EM analysis showed the soluble oligomers as a homogeneous population of small globular structures, free of fibrillar structures (Fig. 1A). The fibrillar A$\beta_{1\text{-}42}$ samples showed long threads measuring $>$1 μm in length (see Fig. 1A). In addition, the fibrillar A$\beta_{1\text{-}42}$ preparations have an $\sim$10-fold higher ThT-binding capacity than the A$\beta_{1\text{-}42}$ oligomers, showing the higher β-sheet content of fibrillar A$\beta_{1\text{-}42}$ (Fig. 1B). A viability assay was performed with actively dividing HEK293 cells, as well as with differentiated SK-N-SH cells, to compare the toxic properties of the A$\beta_{1\text{-}42}$ preparations. The cells were treated with 10 μM oligomeric or fibrillar A$\beta_{1\text{-}42}$ for 48 h. Oligomeric A$\beta_{1\text{-}42}$ was significantly more toxic to both cell types than was fibrillar A$\beta_{1\text{-}42}$ with the MTT viability assay (Fig. 1C and D). The effect of A$\beta_{1\text{-}42}$ was less pronounced for the HEK293 cells, most likely because of proliferation during the incubation. A$\beta_{42\text{-}1}$ had no effect on cell viability (data not shown). TUNEL staining shows more positive nuclei in SK-N-SH cells treated with oligomeric than with fibrillar A$\beta_{1\text{-}42}$, indicating increased apoptosis (Fig. 1E). Our results confirm the structural and biologic properties of the oligomeric and fibrillar A$\beta_{1\text{-}42}$ preparations, as previously described (1, 12, 14) and thus provide a valid model to study effects of Aβ aggregation state.

A$\beta_{1\text{-}42}$ does not affect overall BiP levels

To determine whether extracellular A$\beta_{1\text{-}42}$ can induce the UPR, BiP levels were analyzed in differentiated SK-N-SH cells after treatment with oligomeric A$\beta_{1\text{-}42}$, fibrillar A$\beta_{1\text{-}42}$, or reverse A$\beta_{1\text{-}42}$ for 48 h (Fig. 2A and B). Tunicamycin, an inhibitor of N-glycosylation in the ER, was used as a positive control for UPR induction. Treatment with 0.2-μg/ml tunicamycin induces BiP levels $\sim$2.5-fold, as expected (see Fig. 2A and B). In contrast, we found no upregulation of BiP with any of the A$\beta_{1\text{-}42}$ preparations. The same result was obtained after prolonging the treatment with A$\beta_{1\text{-}42}$ to 4 days (see Fig. 2C and D). Because upregulation of BiP is an obligatory consequence of UPR activation, these data indicate that A$\beta_{1\text{-}42}$ does not in-

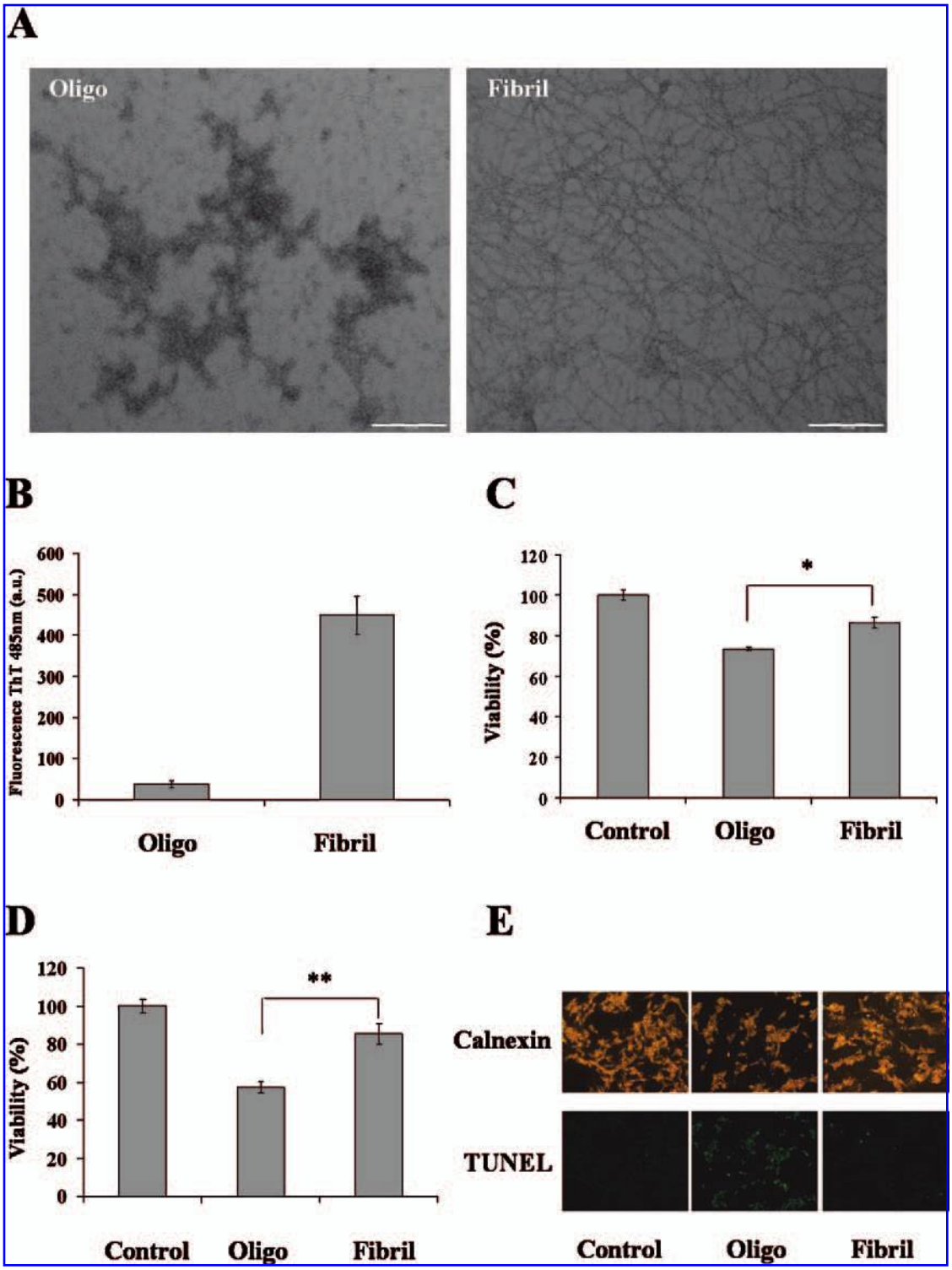

FIG. 1. Characterization of enriched oligomeric and fibrillar A$\beta_{1\text{-}42}$ preparations. Preparations enriched in oligomeric (Oligomers) and fibrillar (Fibrils) A$\beta_{1\text{-}42}$ were prepared as described in Materials and Methods. (**A**) Representative electron-microscope images of oligomeric and fibrillar preparations of A$\beta_{1\text{-}42}$ (scale bar, 200 nm) with negative stain. (**B**) ThT assay performed on the oligomeric (Oligo) and fibrillar (Fibril) Aβ preparations. Graph represents the mean ± SD for $n = 15$ from triplicate wells from five separate experiments using oligomeric or fibrillar enriched A$\beta_{1\text{-}42}$ preparations. (**C**) HEK 293 cells or (**D**) SK-N-SH cells differentiated for 5 days were treated without A$\beta_{1\text{-}42}$ (Control) or with 10 μM oligomeric or fibrillar A$\beta_{1\text{-}42}$ for 48 h. Viability of the cells was determined by MTT assay and is depicted as percentage of control. The graphs represent the mean ± SD for $n = 9$ from triplicate wells from three independent experiments using different A$\beta_{1\text{-}42}$ preparations. *$p < 0.005$; **$p < 0.001$. (**E**) SK-N-SH cells were treated as in **D,** and TUNEL staining was performed to assess apoptosis; calnexin was used as counterstain. (For interpretation of the references to color in this figure legend, the reader is referred to the web version of this article at www.liebertonline.com/ars)

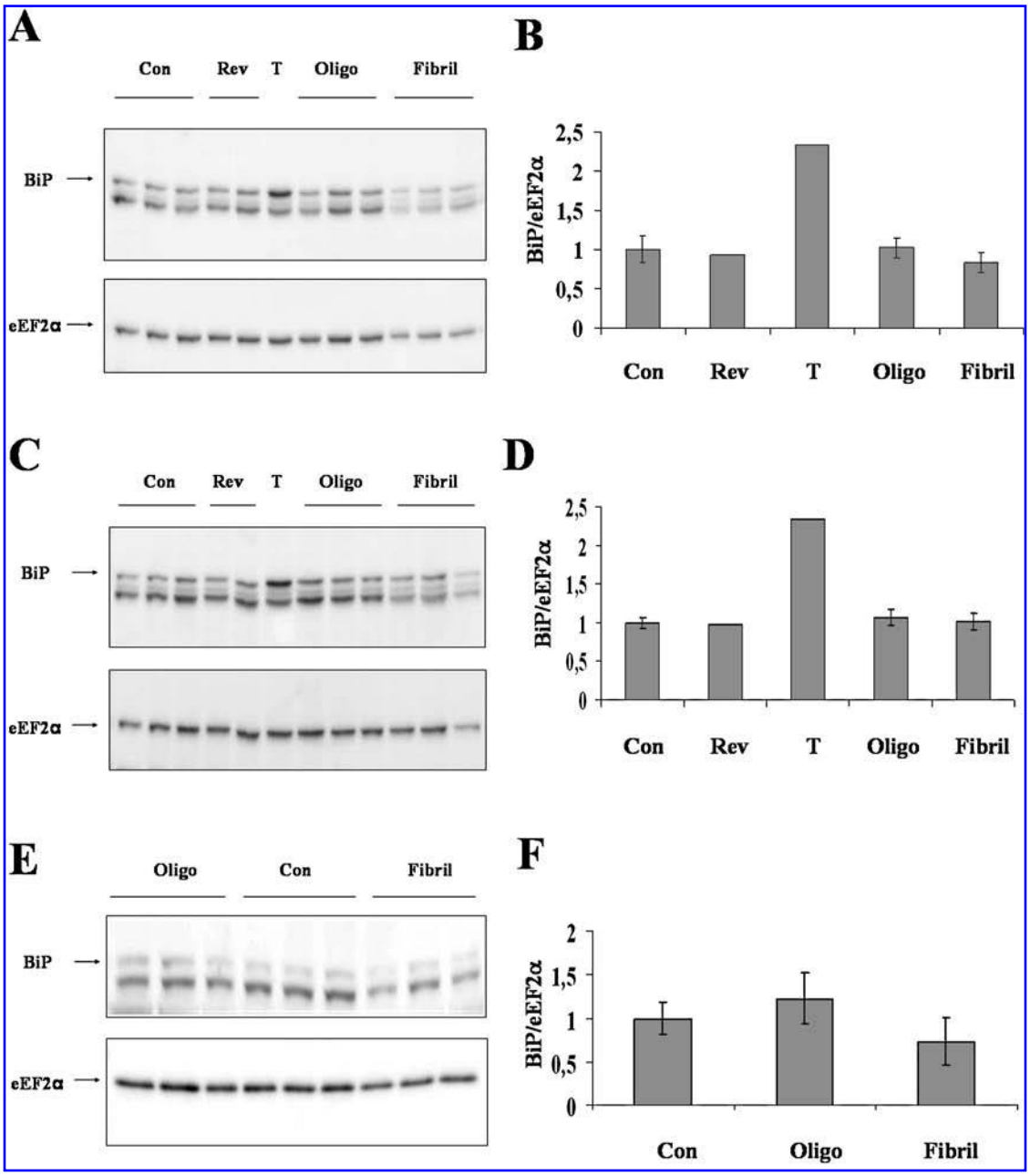

FIG. 2. A$\beta_{1\text{-}42}$ does not induce BiP levels, irrespective of its aggregation state. Western blot analysis of BiP levels in cells incubated without A$\beta_{1\text{-}42}$ (Con), or in the presence of 0.2 μg/ml tunicamycin (T), 10 μM oligomeric (Oligo), fibrillar (Fibril) or reverse (Rev) A$\beta_{1\text{-}42}$. The top band (*arrow*) is BiP; the lower band is cross-reactivity with Hsc70; eEF2α was used as loading control. (**A**) Differentiated SK-N-SH cells treated for 48 h with A$\beta_{1\text{-}42}$; tunicamycin treatment was 24 h. (**B**) Quantification performed on the Western blot shown in (**A**). (**C**) Differentiated SK-N-SH cells treated for 5 days with A$\beta_{1\text{-}42}$; tunicamycin treatment was 24 h. (**D**) Quantification performed on the Western blot shown in **C**. (**E**) Western-blot analysis of BiP levels in HEK293 cells incubated for 48 h without Aβ (control), or in the presence of 10 μM oligomeric (Oligo) or fibrillar (Fibril) A$\beta_{1\text{-}42}$. The top band (*arrow*) is BiP; the lower band is crossreactivity with Hsc70; eEF2α was used as loading control. (**F**) Graph of the quantification performed on the Western blot shown in **E.**

duce an ER stress response in this experimental setup. To exclude possible cell-specific effects, we also analyzed the BiP levels in HEK293 cells treated with A$\beta_{1\text{-}42}$. These cells respond to A$\beta_{1\text{-}42}$ in a similar way to SK-N-SH cells: Neither oligomeric nor fibrillar A$\beta_{1\text{-}42}$ results in upregulation of BiP levels (Fig. 2E and F).

A$\beta_{1\text{-}42}$ oligomers, but not fibrils, induce low-level ER stress

It is possible that extracellular Aβ perturbs ER homeostasis in a more subtle manner that is not detected by analysis of protein levels in a pool of cells. Therefore, we used a HEK293 flu-

orescent ER-stress reporter cell line (ERAI) based on XBP splicing (1). This allows analysis of ER stress in individual cells and could therefore provide a readout in case only low-level ER stress is induced in a relatively small fraction of the cell population. The ERAI cell line responds to ER stress by a fluorescent signal (YFP) that increases with increasing concentrations of tunicamycin (Fig. 3A). The specificity of the reporter for ER stress is demonstrated by treatment of ERAI cells with either tunicamycin or the proteasome inhibitor epoxomycin. The latter treatment does not result in an ER stress response, as shown by absence of BiP induction, but does induce the cytosolic heat-shock stress response, indicated by induction of Hsp70 (see Fig. 3B). This is opposite to treatment with tunicamycin, which induces the ER stress response, shown by induction of BiP, but not the cytosolic stress response (see Fig. 3B). The ERAI cells become fluorescent with tunicamycin, but not with epoxomycin (see Fig. 3C), showing the specificity of the reporter for ER stress.

The level of fluorescence increases with increasing tunicamycin concentration (Fig. 3A and Table 1). This is caused by a higher number of fluorescent cells (total fluorescence, Table 1), as well as a shift to higher intensity per cell (relative intensity distribution; Fig. 4B). At a mild ER stress–inducing concentration (0.1 μg/ml) of tunicamycin, the population of cells with low-level fluorescence intensity contributes most to the total level of fluorescence, whereas with increasing concentrations of tunicamycin, the contribution of the population with medium and higher fluorescence intensity increases.

ERAI cells were treated with 10 μM oligomeric or fibrillar $A\beta_{1\text{-}42}$. Treatment with oligomeric preparations of $A\beta_{1\text{-}42}$ induces ER stress in the ERAI cells (Fig. 4A), albeit not very potently. Not every cell shows fluorescence, and the total level of fluorescence is less than that induced by tunicamycin treatment (see Table 1). The fluorescent signal was observed after treatment with $A\beta_{1\text{-}42}$ for 24 h (data not shown), but was stronger at 48 h (sevenfold higher than untreated cells; Table 1), indicating a relatively slow response. Interestingly, treatment with an equal amount of fibrillar $A\beta_{1\text{-}42}$ does not lead to an ER stress response, suggesting that it is an effect mediated specifically by nonfibrillar $A\beta$. Treatment with the reverse $A\beta_{42\text{-}1}$ also does not induce an ER stress response (data not shown), indicating that not just any nonfibrillar 42-mer induces ER stress. The fluorescence-intensity distribution in oligomer-treated cells is similar to the mild ER stress–inducing concentration (0.1 μg/ml) of tunicamycin, with which the low-fluorescence-intensity population contributes ~70% to total fluorescence (see Fig. 4B). These data suggest that $A\beta_{1\text{-}42}$ induces low-level ER stress in an aggregation state-dependent manner.

UPR induction contributes to oligomer-specific $A\beta_{1\text{-}42}$ toxicity

To study the functional implications of mild UPR induction by oligomeric $A\beta_{1\text{-}42}$, we tested whether ER stress induction sensitizes cells for $A\beta$-induced toxicity. To this end, differentiated SK-N-SH cells were treated with $A\beta_{1\text{-}42}$ in the presence of 0.1 μg/ml tunicamycin. This concentration of tunicamycin

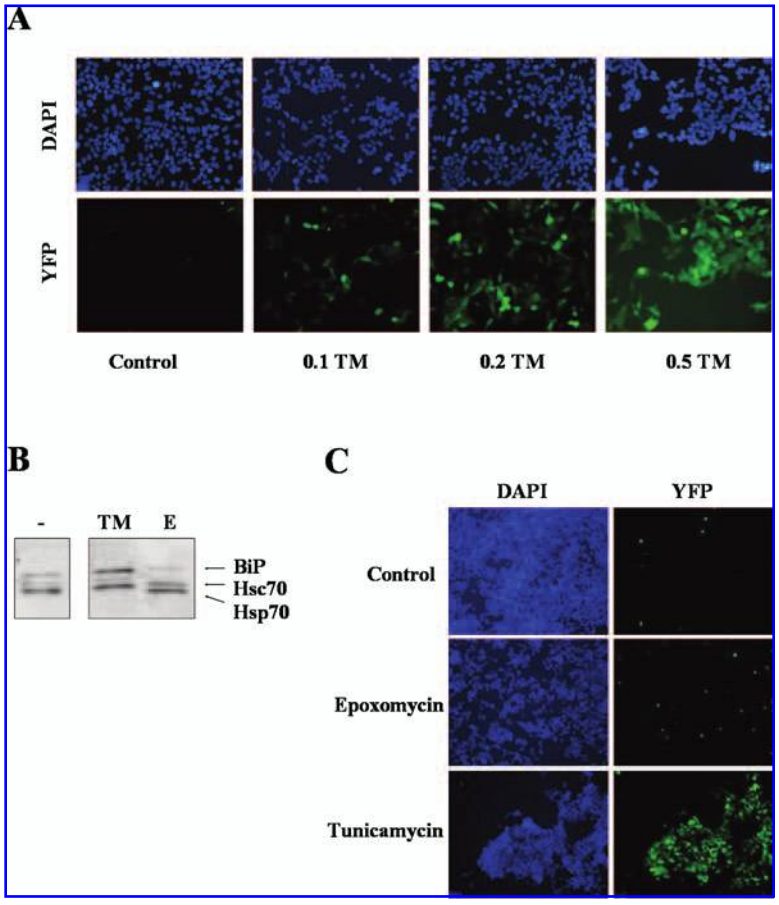

FIG. 3. ERAI is an ER stress–specific reporter. (**A**) HEK293 ERAI cells were treated with increasing tunicamycin concentrations for 24 h. Shown are representative fluorescence pictures: *top panel*, DAPI staining of the nuclei; *bottom panel*, the YFP signal of the ER stress reporter. (**B**) Western-blot analysis of BiP levels in differentiated SK-N-SH cells treated with 0.2 μg/ml tunicamycin or 100 nM epoxomycin for 24 h. The antibody recognizes several Hsp70 proteins: top band (*arrow*) is BiP, the middle band is cross-reactivity with Hsc70, and the lower band is visible only in the epoxomycin-treated sample is Hsp70. (**C**) HEK293 ERAI cells were treated with 0.2 μg/ml tunicamycin or 100 nM epoxomycin for 24 h. Shown are representative fluorescence pictures: *left panel*, DAPI staining of the nuclei; *right panel*, the YFP signal of the ER-stress reporter. (For interpretation of the references to color in this figure legend, the reader is referred to the web version of this article at www.liebertonline.com/ars)

TABLE 1. QUANTIFICATION OF FLUORESCENT SIGNAL CORRECTED FOR CELL NUMBER IN HEK293 ERAI CELLS AFTER TREATMENT WITHOUT (CONTROL) OR WITH 0.1, 0.2, AND 0.5 μG/ML TUNICAMYCIN (TM) FOR 24 H OR WITH OLIGOMERIC (OLIGO) OR FIBRILLAR (FIBRIL) Aβ FOR 48 H

	Mean ± SD
Control	11 ± 9
0.1 TM	176 ± 60
0.2 TM	604 ± 206
0.5 TM	1,441 ± 703
Oligo	71 ± 40
Fibril	10 ± 10

Numbers represent mean ± SD of normalized YFP fluorescence signal (arbitrary units) from 12 to 25 images from three different experiments. See materials and methods for details.

mildly induces the UPR in these cells (8), but does not result in a (significant) reduction of viability (Fig. 5A). To facilitate analysis of interactions of ER stress and A$\beta_{1\text{-}42}$ toxicity, a lower and less-toxic concentration of A$\beta_{1\text{-}42}$ (1 μM) was used. Treatment with 1 μM oligomeric and fibrillar A$\beta_{1\text{-}42}$ reduces the viability to 70% and 90%, respectively, showing that the differential effect of oligomers and fibrils on cell viability is also observed using this concentration (see Fig. 5A). Co-incubation of tunicamycin with fibrillar A$\beta_{1\text{-}42}$ did not result in decreased viability (see Fig. 5A). In contrast, oligomeric A$\beta_{1\text{-}42}$ induces a significant reduction in cellular viability in the presence of tunicamycin (see Fig. 5A). This increased sensitization for oligomer toxicity suggests that A$\beta_{1\text{-}42}$ oligomers and tunicamycin have a common mechanism of toxicity. This result indicates that induction of the UPR contributes specifically to the toxicity of oligomeric A$\beta_{1\text{-}42}$ but not to the toxicity of fibrillar A$\beta_{1\text{-}42}$. This, at least in part, involves an apoptotic process, because increased TUNEL staining is observed in oligomer/tunicamycin–treated cells, but not in fibril/tunicamycin–treated cells (see Fig. 5B), thus reflecting the viability data. ER stress could thus be one of the molecular mechanisms involved in oligomer-specific Aβ toxicity.

DISCUSSION

In the present study, we investigated whether extracellular Aβ can be involved in induction of the UPR, as well as the possible role of the conformational state of Aβ on UPR activation. To this end, we made preparations enriched in oligomeric or fibrillar forms of A$\beta_{1\text{-}42}$. Analysis by EM and ThT assay showed that these preparations have the structural properties of oligomeric and fibrillar Aβ aggregates. In addition, oligomeric A$\beta_{1\text{-}42}$ is significantly more toxic than A$\beta_{1\text{-}42}$ fibrils, which reflects the biologic properties of Aβ aggregates, as previously reported by others (1, 12, 14).

In two different cell types (differentiated SK-N-SH and HEK293 cells), we determined the levels of the ER stress indicator BiP after treatment with A$\beta_{1\text{-}42}$. In this experimental

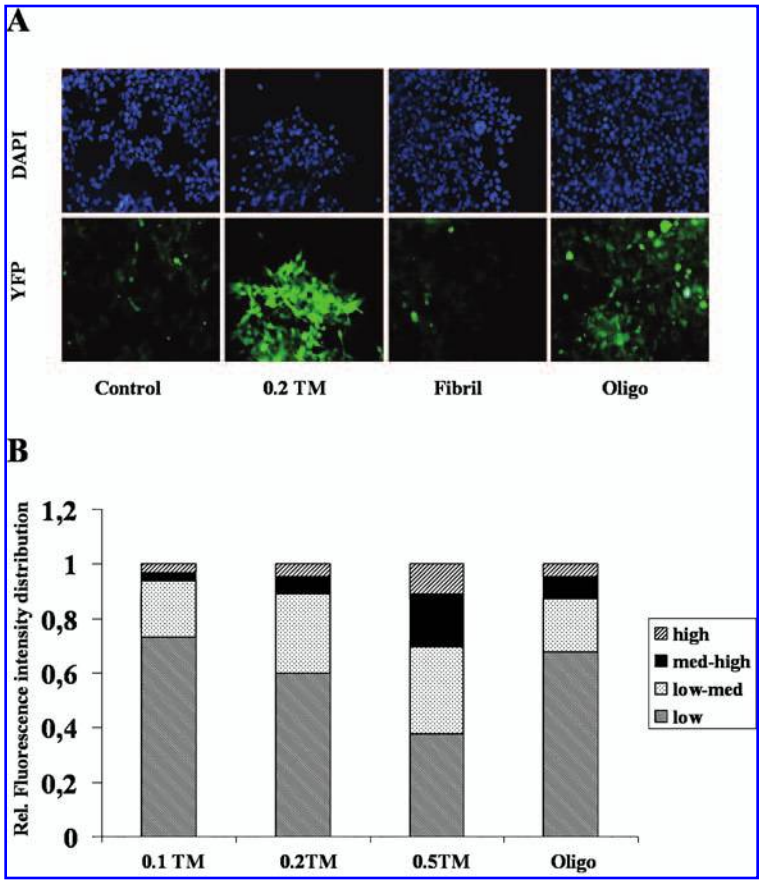

FIG. 4. Mild UPR induction by A$\beta_{1\text{-}42}$ is dependent on its aggregation state. (**A**) ERAI293 ER-stress reporter cells were incubated without Aβ (control) or in the presence of 10 μM oligomeric (Oligomers) or fibrillar (Fibrils) preparations of A$\beta_{1\text{-}42}$ for 48 h. Treatment with 0.2 μg/ml tunicamycin (TM) for 24 h is shown as positive control. Shown are representative fluorescence pictures from a representative experiment. In the top panel, DAPI staining of the nuclei; in the bottom panel, the YFP signal of the ER-stress reporter. (**B**) Distribution of the fluorescence intensity in HEK293 ERAI cells after treatment with 0.1-, 0.2-, and 0.5-μg/ml tunicamycin (TM) for 24 h or 10 μM oligomeric (Oligo) A$\beta_{1\text{-}42}$ for 48 h. See Materials and Methods for details. (For interpretation of the references to color in this figure legend, the reader is referred to the web version of this article at www.liebertonline.com/ars)

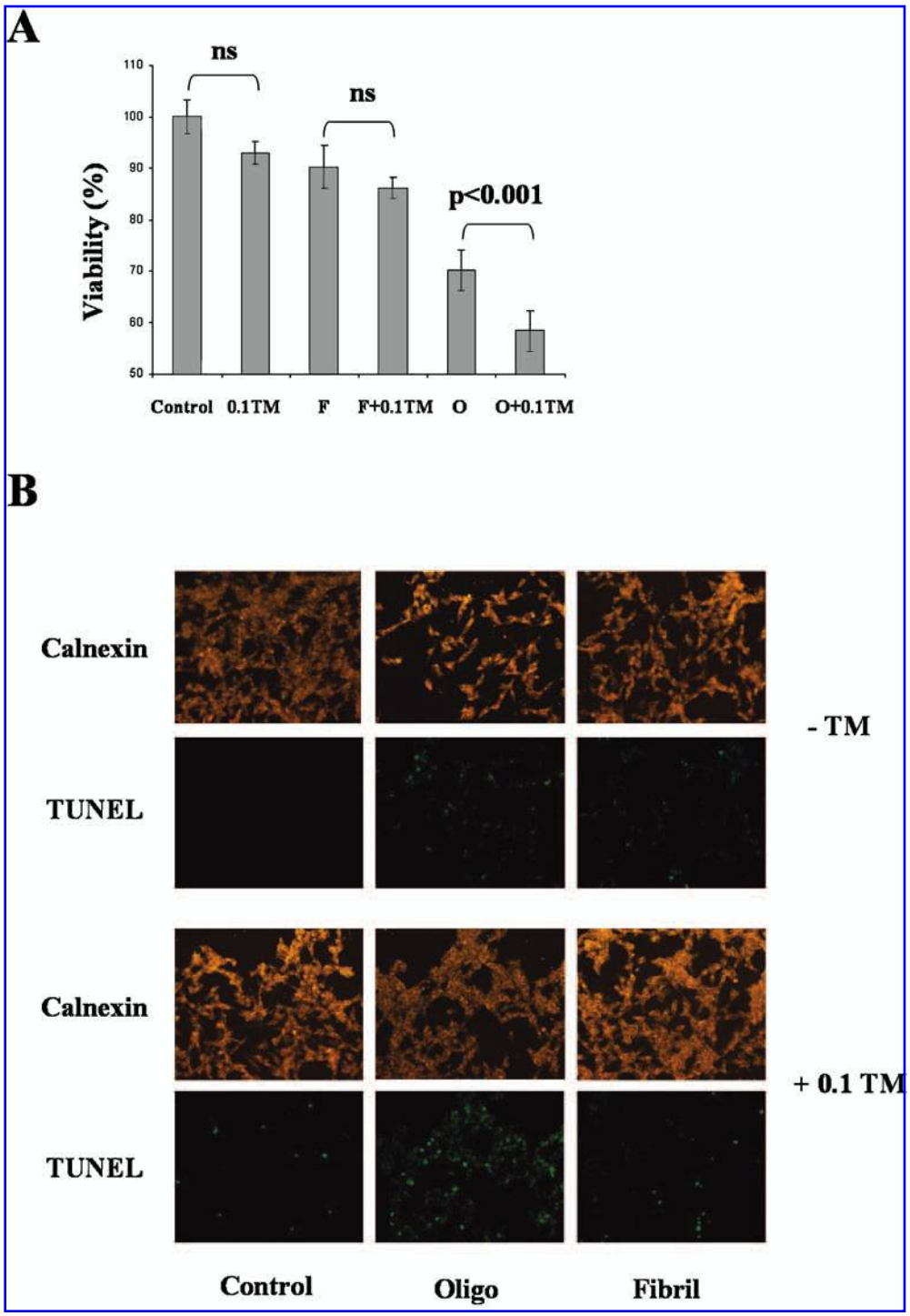

FIG. 5. ER-stress induction sensitizes cells specifically for oligomeric A$\beta_{1\text{-}42}$ toxicity. SK-N-SH cells were differentiated for 5 days before co-incubation for 48 h with 0 or 0.1 μg/ml tunicamycin (0.1 TM), and 1 μM oligomeric (O) or fibrillar (F) preparations of A$\beta_{1\text{-}42}$. (**A**) Viability of the cells was determined by MTT assay and is depicted as percentage of control (untreated cells). The graphs represent the mean ± SD for $n = 6$ from triplicate wells from two independent experiments using different A$\beta_{1\text{-}42}$ preparations. (**B**) TUNEL staining of SK-N-SH cells treated as in **A.** Calnexin was used as counterstain. (For interpretation of the references to color in this figure legend, the reader is referred to the web version of this article at www.liebertonline.com/ars)

setup, we found no evidence for UPR induction by extracellular A$\beta_{1\text{-}42}$, irrespective of the aggregation state, cell type, or duration of treatment. Using a fluorescent ER stress indicator that allows analysis of individual cells, we demonstrated that extracellular application of oligomer-enriched preparations of A$\beta_{1\text{-}42}$ causes an induction of the UPR, whereas fibrillar A$\beta_{1\text{-}42}$ does not. The fluorescent ER stress-reporter signal is induced sevenfold by oligomeric A$\beta_{1\text{-}42}$; the total level of fluo-

rescence is ~2.5 times lower than in cells treated with 0.1 μg/ml tunicamycin. In addition, we found that in the oligomer-treated cells, the low-level ER stress population contributes most to the total fluorescence level, comparable to cells treated with 0.1 μg/ml tunicamycin. This indicates that oligomeric A$\beta_{1\text{-}42}$ induces a mild ER stress response. This subtle induction of the UPR in a fraction of the cells will be diluted out using biochemical analysis and could explain why we do not find induction of BiP levels by A$\beta_{1\text{-}42}$ on Western blot.

Previously, mild induction of BiP levels by a fragment of Aβ, A$\beta_{25\text{-}35}$, has been reported (18, 22). A$\beta_{25\text{-}35}$ is often used as "toxic fragment" in *in vitro* studies, but does not naturally occur in human brain, unlike the full-length A$\beta_{1\text{-}42}$ used in this study. A$\beta_{25\text{-}35}$ lacks the peptide domains critical for fibril formation, which would fit with our observation that only nonfibrillar A$\beta_{1\text{-}42}$ induces ER stress. Although UPR activation results in increased BiP levels, increased BiP is not necessarily the result of UPR induction. Aβ was reported to cause apoptosis by activation of ER-stress–specific caspases (6, 16), but induction of the UPR by Aβ was not shown in these studies. The reporter used in our study is based on the unconventional splicing of XBP1 mRNA that is specific for the UPR and thus provides the first direct evidence for UPR activation by A$\beta_{1\text{-}42}$. Because XBP1 splicing is downstream of Ire1 signaling, we cannot fully rule out that Aβ affects the splicing in an ER-stress–independent manner. However, this seems very unlikely, because the splicing of XBP1 mRNA involves a different machinery than the conventional pre-mRNA splicing and is activated only by ER stress. In a recent study, Aβ-induced apoptosis was found to be independent of an unfolded protein response (21). Our study indicates that enriched oligomeric preparations of A$\beta_{1\text{-}42}$ are needed to cause an induction of ER stress. In the study by Yu *et al*. (21), a more fibrillar Aβ preparation was used, which may explain why no ER stress induction was found. In addition, the low level of ER stress we report in this study is found only using the fluorescent reporter system that allows detection of low-level ER stress in only part of a cell population.

Oligomeric A$\beta_{1\text{-}42}$ induces only mild ER stress, but that does not imply that it has no functional implications. Long-term exposure to a mild toxic stimulus, which is likely to be the case for Aβ exposure of AD neurons, may be just as deleterious as short exposure to a strong toxic stimulus. Combination with additional toxic factors may increase the stress in the ER. This is illustrated by the observation that ER stress–mediated toxicity is potentiated more by oligomeric than by fibrillar A$\beta_{1\text{-}42}$. This increased sensitivity to oligomer toxicity indicates that A$\beta_{1\text{-}42}$ oligomers and tunicamycin have a common mechanism of toxicity. This suggests that ER stress is involved in oligomer-specific toxicity, at least to a larger extent than in fibril-specific toxicity.

How extracellular Aβ would signal to the ER is unknown. One possible mechanism is that extracellular Aβ induces a signaling cascade that extends to the ER, possibly *via* Ca^{2+}. Previous studies have shown that Aβ triggers the release of Ca^{2+} from the ER in neurons (4, 10, 18). Disturbance of ER Ca^{2+} homeostasis may result in perturbations of ER functioning and induce ER stress. Interestingly, oligomeric Aβ specifically has been shown to cause this release of Ca^{2+} from the ER (2). Whether the oligomer-specific induction of ER stress, found in this study, is caused by disturbed Ca^{2+} homeostasis remains to be shown.

Alternatively, Aβ may be internalized and transported to the ER itself. It is possible that the induction of the UPR is found only with oligomeric A$\beta_{1\text{-}42}$, because the more-bulky fibrillar A$\beta_{1\text{-}42}$ is not so easily internalized. This may also explain why only small fragments of Aβ have previously been reported to induce BiP levels (18, 22). The presence of aggregated Aβ in the ER may directly interact with the quality-control systems in the ER. An indication that this may be the case is found in sporadic inclusion body myositis (sIBM), a degenerative muscle disease characterized by the formation of intracellular Aβ inclusion bodies (3). Several ER chaperones (including BiP) are upregulated in sIBM, suggesting activation of the UPR (20). Although in this case, Aβ is produced intracellularly, this at least suggests that Aβ can invoke a response of the ER quality-control system.

Different Aβ assembly forms may mediate diverse toxic effects at different stages of the disease (7). For example, the effects of Aβ on synapses were shown to be specifically mediated by oligomeric Aβ *in vitro* (13). This correlates well with the occurrence of synaptic dysfunction early in the pathogenic cascade of AD, before deposition of fibrillar Aβ in plaques. In this study, we showed that extracellular A$\beta_{1\text{-}42}$ in oligomeric form can induce an ER stress response *in vitro*. The association with prefibrillar Aβ would fit with our previous observation that the UPR in AD brain is activated before deposition of fibrillar Aβ (9). Our data also indicate that activation of the UPR contributes to the aggregation state–specific toxicity of oligomeric A$\beta_{1\text{-}42}$. ER stress could thus be an important mechanism of Aβ-induced neuronal loss in AD pathogenesis. A better understanding of the role of ER stress in AD pathology will create the possibility for targeted therapeutic intervention.

ACKNOWLEDGMENTS

We thank Dr. Jan van Marle for assistance with EM analysis, Dr. M. Miura for the gift of the ERAI reporter construct, Ms. María López-Cavanillas for expert technical assistance, and Prof. Piet Eikelenboom for stimulating discussions and critical reading of the manuscript. This work is supported by the Internationale Stichting Alzheimer Onderzoek (ISAO grant 02504 and 05508 to W.S.). W.S. is a fellow of the Anton Meelmeijer Center for Translational Research.

ABBREVIATIONS

Aβ, β-amyloid; AD, Alzheimer disease; EM, electron microscopy; ER, endoplasmic reticulum; PERK, pancreatic ER kinase; sIBM, sporadic inclusion body myositis; MTT, 3-(4,5-dimethylthiazol-2-yl)-2,5-diphenyltetrazolium bromide; ThT, thioflavin T; UPR, unfolded protein response; XBP-1, X-box–binding protein 1; YFP, yellow fluorescent protein.

REFERENCES

1. Dahlgren KN, Manelli AM, Stine WB Jr, Baker LK, Krafft GA, and LaDu MJ. Oligomeric and fibrillar species of amyloid-beta peptides differentially affect neuronal viability. *J Biol Chem* 277: 32046–32053, 2002.

2. Demuro A, Mina E, Kayed R, Milton SC, Parker I, and Glabe CG. Calcium dysregulation and membrane disruption as a ubiquitous neurotoxic mechanism of soluble amyloid oligomers. *J Biol Chem* 280: 17294–17300, 2005.
3. Engel WK and Askanas V. Inclusion-body myositis: clinical, diagnostic, and pathologic aspects. *Neurology* 66: S20–S29, 2006.
4. Ferreiro E, Oliveira CR, and Pereira C. Involvement of endoplasmic reticulum Ca^{2+} release through ryanodine and inositol 1,4,5-triphosphate receptors in the neurotoxic effects induced by the amyloid-beta peptide. *J Neurosci Res* 76: 872–880, 2004.
5. Forman MS, Lee VM, and Trojanowski JQ. "Unfolding" pathways in neurodegenerative disease. *Trends Neurosci* 26: 407–410, 2003.
6. Hitomi J, Katayama T, Eguchi Y, Kudo T, Taniguchi M, Koyama Y, Manabe T, Yamagishi S, Bando Y, Imaizumi K, Tsujimoto Y, and Tohyama M. Involvement of caspase-4 in endoplasmic reticulum stress-induced apoptosis and Abeta-induced cell death. *J Cell Biol* 165: 347–356, 2004.
7. Hoozemans JJ, Chafekar SM, Baas F, Eikelenboom P, and Scheper W. Always around, never the same: pathways of amyloid beta induced neurodegeneration throughout the pathogenic cascade of Alzheimer's disease. *Curr Med Chem* 13: 2599–2605, 2006.
8. Hoozemans JJ, Stieler J, van Haastert ES, Veerhuis R, Rozemuller AJ, Baas F, Eikelenboom P, Arendt T, and Scheper W. The unfolded protein response affects neuronal cell cycle protein expression: implications for Alzheimer's disease pathogenesis. *Exp Gerontol* 41: 380–386, 2006.
9. Hoozemans JJ, Veerhuis R, Rozemuller AJ, Baas F, Eikelenboom P, and Scheper W. The unfolded protein response is activated in Alzheimer's disease. *Acta Neuropathol* (*Berl*) 110: 165–172, 2005.
10. Iuvone T, Esposito G, Esposito R, Santamaria R, Di Rosa M, and Izzo AA. Neuroprotective effect of cannabidiol, a non-psychoactive component from *Cannabis sativa*, on beta-amyloid-induced toxicity in PC12 cells. *J Neurochem* 89: 134–141, 2004.
11. Iwawaki T, Akai R, Kohno K, and Miura M. A transgenic mouse model for monitoring endoplasmic reticulum stress. *Nat Med* 10: 98–102, 2004.
12. Kayed R, Head E, Thompson JL, McIntire TM, Milton SC, Cotman CW, and Glabe CG. Common structure of soluble amyloid oligomers implies common mechanism of pathogenesis. *Science* 300: 486–489, 2003.
13. Klyubin I, Walsh DM, Lemere CA, Cullen WK, Shankar GM Betts V, Spooner ET, Jiang L, Anwyl R, Selkoe DJ, and Rowan MJ. Amyloid beta protein immunotherapy neutralizes Abeta oligomers that disrupt synaptic plasticity in vivo. *Nat Med* 11: 556–561, 2005.
14. Lambert MP, Barlow AK, Chromy BA, Edwards C, Freed R, Liosatos M, Morgan TE, Rozovsky I, Trommer B, Viola KL, Wals P, Zhang C, Finch CE, Krafft GA, and Klein WL. Diffusible, nonfibrillar ligands derived from Abeta1-42 are potent central nervous system neurotoxins. *Proc Natl Acad Sci U S A* 95: 6448–6453, 1998.
15. Mattson MP. Pathways towards and away from Alzheimer's disease. *Nature* 430: 631–639, 2004.
16. Nakagawa T, Zhu H, Morishima N, Li E, Xu J, Yankner BA, and Yuan J. Caspase-12 mediates endoplasmic-reticulum-specific apoptosis and cytotoxicity by amyloid-beta. *Nature* 403: 98–103, 2000.
17. Rutkowski DT and Kaufman RJ. A trip to the ER: coping with stress. *Trends Cell Biol* 14: 20–28, 2004.
18. Suen, KC Lin KF, Elyaman W, So KF, Chang RC, and Hugon J. Reduction of calcium release from the endoplasmic reticulum could only provide partial neuroprotection against beta-amyloid peptide toxicity. *J Neurochem* 87: 1413–1426, 2003.
19. Unterberger U, Hoftberger R, Gelpi E, Flicker H, Budka H, and Voigtlander T. Endoplasmic reticulum stress features are prominent in Alzheimer disease but not in prion diseases in vivo. *J Neuropathol Exp Neurol* 65: 348–357, 2006.
20. Vattemi G, Engel WK, McFerrin J, and Askanas V. Endoplasmic reticulum stress and unfolded protein response in inclusion body myositis muscle. *Am J Pathol* 164: 1–7, 2004.
21. Yu MS, Suen KC, Kwok NS, So KF, Hugon J, and Chuen-Chung Chang R. Beta-amyloid peptides induces neuronal apoptosis via a mechanism independent of unfolded protein responses. *Apoptosis* 11: 687–700, 2006.
22. Yu Z, Luo, H, Fu W, and Mattson MP. The endoplasmic reticulum stress-responsive protein GRP78 protects neurons against excitotoxicity and apoptosis: suppression of oxidative stress and stabilization of calcium homeostasis. *Exp Neurol* 155: 302–314, 1999.

Address reprint requests to:
W. Scheper, Ph.D.
Academic Medical Center
Neurogenetics Laboratory
P.O. Box 22660
1100 DD Amsterdam
The Netherlands

E-mail: w.scheper@amc.uva.nl

Date of first submission to ARS Central, June 20, 2007; date of acceptance, July 1, 2007.

This article has been cited by:

1. Jeroen J.M. Hoozemans, Wiep Scheper. 2012. Endoplasmic reticulum: The unfolded protein response is tangled in neurodegeneration. *The International Journal of Biochemistry & Cell Biology* **44**:8, 1295-1298. [CrossRef]
2. Julie A. Moreno, Helois Radford, Diego Peretti, Joern R. Steinert, Nicholas Verity, Maria Guerra Martin, Mark Halliday, Jason Morgan, David Dinsdale, Catherine A. Ortori, David A. Barrett, Pavel Tsaytler, Anne Bertolotti, Anne E. Willis, Martin Bushell, Giovanna R. Mallucci. 2012. Sustained translational repression by eIF2#-P mediates prion neurodegeneration. *Nature* . [CrossRef]
3. Line Kimpe, Elise S. Haastert, Archontia Kaminari, Rob Zwart, Helma Rutjes, Jeroen J. M. Hoozemans, Wiep Scheper. 2012. Intracellular accumulation of aggregated pyroglutamate amyloid beta: convergence of aging and A# pathology at the lysosome. *AGE* . [CrossRef]
4. Diana AT Nijholt, Elise S van Haastert, Annemieke JM Rozemuller, Wiep Scheper, Jeroen JM Hoozemans. 2012. The unfolded protein response is associated with early tau pathology in the hippocampus of tauopathies. *The Journal of Pathology* n/a-n/a. [CrossRef]
5. Z. Sultana, K.E. Paleologou, K.M. Al-Mansoori, M.T. Ardah, N. Singh, S. Usmani, H. Jiao, F.L. Martin, M.M.S. Bharath, S. Vali, O.M.A. El-Agnaf. 2011. Dynamic modeling of #-synuclein aggregation in dopaminergic neuronal system indicates points of neuroprotective intervention: experimental validation with implications for Parkinson's therapy. *Neuroscience* **199**, 303-317. [CrossRef]
6. Sergio T. Ferreira, William L. Klein. 2011. The A# oligomer hypothesis for synapse failure and memory loss in Alzheimer’s disease. *Neurobiology of Learning and Memory* . [CrossRef]
7. D A T Nijholt, T R de Graaf, E S van Haastert, A Osório Oliveira, C R Berkers, R Zwart, H Ovaa, F Baas, J J M Hoozemans, W Scheper. 2011. Endoplasmic reticulum stress activates autophagy but not the proteasome in neuronal cells: implications for Alzheimer's disease. *Cell Death and Differentiation* **18**:6, 1071-1081. [CrossRef]
8. Jesse C. Wiley, Christina Pettan-Brewer, Warren C. Ladiges. 2011. Phenylbutyric acid reduces amyloid plaques and rescues cognitive behavior in AD transgenic mice. *Aging Cell* **10**:3, 418-428. [CrossRef]
9. Massimo StefaniAmyloid Polymorphisms: Structural Basis and Significance in Biology and Molecular Medicine 121-142. [CrossRef]
10. Teruo Hayashi, Shang-Yi Tsai, Tomohisa Mori, Michiko Fujimoto, Tsung-Ping Su. 2011. Targeting ligand-operated chaperone sigma-1 receptors in the treatment of neuropsychiatric disorders. *Expert Opinion on Therapeutic Targets* 1-21. [CrossRef]
11. István Földi, Zsolt L. Datki, Zoltán Szabó, Zsolt Bozsó, Botond Penke, Tamás Janáky. 2011. Proteomic study of the toxic effect of oligomeric A#1-42 in situ prepared from ‘iso-A#1-42’. *Journal of Neurochemistry* no-no. [CrossRef]
12. Klaudia Jomova, Dagmar Vondrakova, Michael Lawson, Marian Valko. 2010. Metals, oxidative stress and neurodegenerative disorders. *Molecular and Cellular Biochemistry* **345**:1-2, 91-104. [CrossRef]
13. Maria Gregori, Valeria Cassina, Doriano Brogioli, Domenico Salerno, Line Kimpe, Wiep Scheper, Massimo Masserini, Francesco Mantegazza. 2010. Stability of A# (1-42) peptide fibrils as consequence of environmental modifications. *European Biophysics Journal* **39**:12, 1613-1623. [CrossRef]
14. Massimo Stefani. 2010. Biochemical and biophysical features of both oligomer/fibril and cell membrane in amyloid cytotoxicity. *FEBS Journal* **277**:22, 4602-4613. [CrossRef]
15. S.M. Kim, S.Y. Yoon, J.E. Choi, J.S. Park, J.M. Choi, T. Nguyen, D.H. Kim. 2010. Activation of eukaryotic initiation factor-2#-kinases in okadaic acid-treated neurons. *Neuroscience* **169**:4, 1831-1839. [CrossRef]
16. Paulius Cizas, Rima Budvytyte, Ramune Morkuniene, Radu Moldovan, Matteo Broccio, Mathias Lösche, Gediminas Niaura, Gintaras Valincius, Vilmante Borutaite. 2010. Size-dependent neurotoxicity of #-amyloid oligomers. *Archives of Biochemistry and Biophysics* **496**:2, 84-92. [CrossRef]
17. M.L. Spatara, A.S. Robinson. 2010. Transgenic mouse and cell culture models demonstrate a lack of mechanistic connection between endoplasmic reticulum stress and tau dysfunction. *Journal of Neuroscience Research* NA-NA. [CrossRef]
18. Jeroen J.M. Hoozemans, Elise S. van Haastert, Diana A.T. Nijholt, Annemieke J.M. Rozemuller, Piet Eikelenboom, Wiep Scheper. 2009. The Unfolded Protein Response Is Activated in Pretangle Neurons in Alzheimer's Disease Hippocampus. *The American Journal of Pathology* **174**:4, 1241-1251. [CrossRef]

19. Vanessa Villard, Julie Espallergues, Emeline Keller, Tursun Alkam, Atsumi Nitta, Kiyofumi Yamada, Toshitaka Nabeshima, Alexandre Vamvakides, Tangui Maurice. 2008. Antiamnesic and Neuroprotective Effects of the Aminotetrahydrofuran Derivative ANAVEX1-41 Against Amyloid #25–35-Induced Toxicity in Mice. *Neuropsychopharmacology* . [CrossRef]
20. Martin Schröder , Kenji Kohno . 2007. Recent Advances in Understanding the Unfolded Protein Response. *Antioxidants & Redox Signaling* **9**:12, 2241-2244. [Citation] [Full Text PDF] [Full Text PDF with Links]